Altering Substrate Specificity at the Heme Edge of Cytochrome *c* Peroxidase[†]

Sheri K. Wilcox, Gerard M. Jensen, Melissa M. Fitzgerald, Duncan E. McRee, and David B. Goodin*

Department of Molecular Biology, MB8, The Scripps Research Institute, 10666 North Torrey Pines Road, La Jolla, California 92037

Received December 12, 1995; Revised Manuscript Received February 12, 1996[⊗]

ABSTRACT: Two mutants of cytochrome *c* peroxidase (CCP) are reported which exhibit unique specificities toward oxidation of small substrates. Ala-147 in CCP is located near the δ-meso edge of the heme and along the solvent access channel through which H_2O_2 is thought to approach the active site. This residue was replaced with Met and Tyr to investigate the hypothesis that small molecule substrates are oxidized at the exposed δ-meso edge of the heme. X-ray crystallographic analyses confirm that the side chains of A147M and A147Y are positioned over the δ-meso heme position and might therefore modify small molecule access to the oxidized heme cofactor. Steady-state kinetic measurements show that cytochrome *c* oxidation is enhanced 3-fold for A147Y relative to wild type, while small molecule oxidation is altered to varying degrees depending on the substrate and mutant. For example, oxidation of phenols by A147Y is reduced to less than 20% relative to the wild-type enzyme, while V_{max}/e for oxidation of other small molecules is less affected by either mutation. However, the "specificity" of aniline oxidation by A147M, i.e., $(V_{max}/e)/K_m$, is 43-fold higher than in wild-type enzyme, suggesting that a specific interaction for aniline has been introduced by the mutation. Stopped-flow kinetic data show that the restricted heme access in A147Y or A147M slows the reaction between the enzyme and H_2O_2, but not to an extent that it becomes rate limiting for the oxidation of the substrates examined. The rate constant for compound ES formation with A147Y is 2.5 times slower than with wild-type CCP. These observations strongly support the suggestion that small molecule oxidations occur at sites on the enzyme distinct from those utilized by cytochrome *c* and that the specificity of small molecule oxidation can be significantly modulated by manipulating access to the heme edge. These results help to define the role of alternative electron transfer pathways in cytochrome *c* peroxidase and may have useful applications in improving the specificity of peroxidases with engineered function.

The recent introductions of small molecule binding sites into the active site of cytochrome *c* peroxidase (CCP)[1] suggest that it might be possible to redesign this enzyme to achieve the oxidation of novel substrates (Fitzgerald et al., 1994, 1995; McRee et al., 1994). CCP is a yeast mitochondrial enzyme which catalyzes the oxidation of cytochrome *c* (cyt *c*) by H_2O_2 (Yonetani, 1976; Poulos & Finzel, 1984). However, wild-type CCP will also nonspecifically oxidize a number of small molecule electron donors, though at rates that are much slower than that for its natural substrate (DePillis et al., 1991; Jordi & Erman, 1974). Thus, in order to achieve high specificity for an engineered catalyst, it is important to demonstrate how one might restrict the promiscuous oxidation of electron donors by CCP without compromising its intrinsic function. In addition to producing a useful template for a more specific catalyst, information about the mechanism and alternative electron transfer pathways utilized by the enzyme may also be determined.

The mechanism of cyt *c* oxidation by CCP is believed to first involve binding of H_2O_2 to the open axial coordination position on the heme to produce compound ES in which the enzyme is oxidized by 2 equiv over the resting ferric state (Yonetani, 1976). In compound ES, the heme is oxidized to an oxyferryl center, Fe(IV)=O (George, 1952, 1953; Yonetani & Ray, 1965; Yonetani et al., 1966), and Trp-191 is reversibly oxidized to a π-cation radical (Sivaraja et al., 1989; Scholes et al., 1989; Erman et al., 1989; Houseman et al., 1993; Huyett et al., 1995; Jensen et al., 1996). Compound ES is reduced back to the resting state upon sequential oxidation of two molecules of its presumed physiological substrate, cyt *c*. Sites for the oxidation of cyt *c* on the surface of CCP have been proposed near the heme γ-meso edge between the heme propionates (Poulos & Kraut, 1980) and more recently near the Trp-191 radical site (Pelletier & Kraut, 1992). Recent data have shown the existence of two distinct sites on CCP for binding by cyt *c* (Stemp & Hoffman, 1993; Zhou & Hoffman, 1994; Wang & Margoliash, 1995; Zhou et al., 1995).

A similar mechanism may operate for the CCP catalyzed oxidation of a number of small molecule electron donors, but it is likely that the sites on the enzyme that are utilized by these substrates are different from those utilized by cyt *c*. The δ-meso heme edge of CCP is partially exposed to solvent through the H_2O_2 access channel leading from the surface of the enzyme to the distal heme face. It has been proposed that oxidations of guaiacol and ferrocyanide require approach to this edge of the heme (DePillis et al., 1991; Ortiz

[†] This research was supported by NIH Grants GM41049 to D.B.G. and GM48495-S1 and GM44841 to D.E.M.

[⊗] Abstract published in *Advance ACS Abstracts,* April 1, 1996.

[1] Abbreviations: CCP, cytochrome *c* peroxidase; CCP(MKT), cytochrome *c* peroxidase produced by expression in *Escherichia coli* containing Met-Lys-Thr at the N-terminus, Ile at position 53, and Gly at position 152; cyt *c*, cytochrome *c*; EPR, electron paramagnetic resonance; compound ES, the H_2O_2 oxidized state of CCP; A147M, mutant in which Ala-147 is replaced by Met; A147Y, mutant in which Ala-147 is replaced by Tyr; MPD, 2-methyl-2,4-pentanediol.

0006-2960/96/0435-4858$12.00/0

de Montellano, 1992). CCPs that contained hemes which were modified by substituents at the δ-meso position were largely inactive toward guaiacol and ferrocyanide oxidations but retained significant activity toward cyt *c*. These results indicated that the heme substituents blocked the site of small substrate interaction with the enzyme but left the sites for interaction with cyt *c* intact. However, it is also possible that the covalent modification of the heme cofactor may have altered its electronic properties, resulting in the observed differences in reactivity.

A structural probe in which direct modification of the heme cofactor could be avoided would provide a more stringent test of the multisite hypothesis. The above studies suggest that introducing steric hindrance into the solvent-accessible channel leading to the δ-meso heme edge by altering the protein structure might modify the specificity of small substrate oxidation. In this paper, we describe the design, construction, and structural characterization of two such mutants. Kinetic data are presented for the reaction of these mutants with H_2O_2 and for their steady-state oxidation of cyt *c* and a number of small molecule electron donors.

MATERIALS AND METHODS

CCP Expression and Purification from Escherichia coli. A147M and A147Y mutants were constructed by oligonucleotide site-directed mutagenesis of single-stranded DNA containing uracil as described previously (Goodin & McRee, 1993). Expression of CCP(MKT), A147M, and A147Y from *E. coli* (Fitzgerald et al., 1994) and purification of these proteins (Goodin et al., 1991) were carried out as described previously. Molar absorptivities at 408 nm ($\epsilon = 101.2$ mM^{-1} cm^{-1} for CCP(MKT), $\epsilon = 96.1$ mM^{-1} cm^{-1} for A147M, and $\epsilon = 96.7$ mM^{-1} cm^{-1} for A147Y) as determined by pyridine hemochromogen assays (Nicola et al., 1975) were used to calculate the protein concentrations from UV−vis absorption spectra.

Spectroscopy. UV−vis spectra were collected at 25 °C in 100 mM potassium phosphate, pH 6.0, using a Hewlett-Packard 8452A or 8453 diode-array spectrophotometer. Compound ES was formed by adding 1.5 equiv of H_2O_2 to 10 μM enzyme in 100 mM potassium phosphate, pH 6.0. The rate of decay of compound ES was measured by adding 8 μM H_2O_2 to 10 μM enzyme and observing the change in absorbance at 424 nm. Electron paramagnetic resonance (EPR) samples were prepared by mixing 450 μM enzyme in 100 mM potassium phosphate, pH 6.0, and 50% glycerol with an ~3-fold molar excess of H_2O_2 in the EPR tube. Freeze−quench EPR samples were prepared by mixing 600 μM enzyme in 100 mM potassium phosphate, pH 6.0, with 600 μM H_2O_2 in a modified Hi-Tech Scientific SHU stopped-flow spectrophotometer. The solution was frozen within 100 ms of mixing by spraying the mixture through a crimped syringe needle directly into a liquid N_2−isopentane bath. The resulting snow was packed into 3-mm quartz tubes. All EPR spectra were collected at X-band on a Bruker ESP300 spectrometer equipped with an Air Products LTR-3 liquid helium cryostat. Temperature was measured with a GaAs diode calibrated to ±0.1 K.

Steady-State Kinetics. CCP displays nonhyperbolic kinetics with respect to cyt *c* concentration (Kang et al., 1977, 1978; Kang & Erman, 1982; Kim et al., 1990), precluding the determination of simple k_{cat} and K_m values from a range of cyt *c* concentrations. Therefore, cyt *c* kinetics were evaluated over a range of H_2O_2 concentrations (Kang & Erman, 1982; Goodin et al., 1987, 1991). Kinetics of cyt *c* oxidation were measured by incubating enzyme (250 pM) with >99% reduced cyt *c* from horse heart (25 μM) and H_2O_2 (10.2−128 μM) in 20 mM Tris/phosphate, pH 6.0 (Goodin et al., 1991). The background rate of cyt *c* oxidation was measured for 30 s and determined to be negligible. The rates were determined from the loss of absorbance at 550 nm, using $\Delta\epsilon_{550} = 18.5$ mM^{-1} cm^{-1} (Margoliash & Frohwirt, 1959). Ferrocyanide oxidation kinetics were measured by incubating enzyme (90 nM wild type, 81 nM A147M, and 81 nM A147Y) with ferrocyanide (0.25−10 mM) and H_2O_2 (170 μM) in 50 mM potassium phosphate buffer, pH 6.0. The rate of ferricyanide formation was determined from the increase in absorbance at 420 nm using $\Delta\epsilon_{420} = 1.02$ mM^{-1} cm^{-1} (Schellenberg & Hellerman, 1958). The background rate was subtracted from the final rate. For ferricyanide and cyt *c*, two molecules of substrate were oxidized for every molecule of enzyme turned over, and therefore the reported V_{max}/e values were adjusted to reflect enzyme turnover. Guaiacol (2-methoxyphenol) oxidation kinetics were measured by incubating enzyme (500 nM) with guaiacol (0.2−75 mM) and H_2O_2 (170 μM) in 50 mM potassium phosphate buffer, pH 6.0. The background rate of guaiacol oxidation was negligible. The rate of formation of tetraguaiacol was measured at 470 nm ($\epsilon = 26.6$ mM^{-1} cm^{-1}) (DePillis et al., 1991). The kinetics of guaiacol oxidation were measured for three separate experiments and averaged. The oxidation of pyrogallol (1,2,3-trihydroxybenzene) was measured using a protocol provided by the Sigma Chemical Co., St. Louis, MO [modification of a procedure by Chance and Maehly (1955)]. H_2O_2 (170 μM) and pyrogallol (4−80 mM) were preequilibrated in 100 mM potassium phosphate buffer, pH 6.0, until there was no change in absorbance. Enzyme (50 nM) was added, and the rate of purpurogallin formation was measured at 420 nm ($\epsilon = 2.64$ mM^{-1} cm^{-1}). Aniline oxidation kinetics were measured by incubating enzyme (1 μM) with aniline (0.1−50 mM) and H_2O_2 (>170 μM) in 100 mM potassium phosphate buffer, pH 6.0. The background rate for aniline oxidation was negligible. The rate of product formation was monitored at 308 nm. Mesidine (2,4,6-trimethylaniline) oxidation kinetics were measured by incubating enzyme (1 μM) with mesidine (0.06−0.6 mM) and H_2O_2 (170 μM) in 100 mM potassium phosphate buffer, pH 6.0. The background rate for mesidine oxidation was negligible. The rate of product formation was monitored at 560 nm. K_m and V_{max}/e values were determined from Eadie−Hofstee plots. Since the nature and molar absorptivities of the products in the oxidations of aniline and mesidine are not well characterized, values proportional to V_{max}/e are reported in terms of s^{-1} mM^{-1}.

X-ray Crystallographic Analysis. Single crystals of CCP mutants were grown from 25% 2-methyl-2,4-pentanediol (MPD) by vapor diffusion (Wang et al., 1990). A147M was crystallized in sitting drops with approximately 0.17 mM enzyme, 33−80 mM potassium phosphate, pH 6, and 10% MPD equilibrated against 25% MPD. A147Y was crystallized in sitting drops with approximately 0.17 mM enzyme, 17−64 mM potassium phosphate, pH 6, and 10% MPD equilibrated against 25% MPD. X-ray diffraction data were collected at 15 °C using Cu Kα radiation from the rotating anode of a Rigaku X-ray generator and a Siemens area

detector. Data were processed using the Xengen suite of programs (Howard et al., 1985). Data were analyzed by difference Fourier techniques using the Scripps XtalView software (McRee, 1992). $|F_{mutant}| - |F_{WT}|$ difference Fourier maps were created for each mutant against the CCP(MKT) structure (Protein Data Base entry 1CCA; Goodin & McRee, 1993). Models were built using XtalView and refined using repeated cycles of manual adjustment with positional and *B*-factor refinements using the program X-PLOR (Brünger et al., 1987).[2]

Stopped-Flow Kinetics. Transient kinetics for the formation of compound ES upon mixing CCP with H_2O_2 were measured at 25 °C on a Hi-Tech Scientific SHU stopped-flow single-wavelength spectrophotometer interfaced to a Hewlett-Packard 9000 computer using a 100-μs photomultiplier time constant. Solutions were equilibrated in the loading syringes 15 min prior to mixing. Absorption kinetics were determined at 424 nm on 1 μM solutions of CCP and 2.5−10 μM solutions of H_2O_2 in 100 mM potassium phosphate, pH 6.0, over a 0.1-s time range (Goodin et al., 1991). Three to five measurements were averaged for each set of conditions. Consistent with earlier reports (Balny et al., 1987), compound ES formation in CCP was observed to be biphasic with a $[H_2O_2]$-dependent fast phase and a much slower $[H_2O_2]$-independent phase. This behavior has been proposed to be the result of an equilibrium between 5- and 6-coordinate forms of the enzyme. The fast phase was of primary interest to this study and was obtained as follows. Since the fast and slow phases were well separated over the range of $[H_2O_2]$ used, the traces could be analyzed by fitting to the equation for $A_t = C(1 - e^{-k_{obs}t}) + Mt + B$ for t = 0−40 ms. In these fits, the slow $[H_2O_2]$-independent phase is approximated by the linear slope M which was determined for a trace at high $[H_2O_2]$. This value of M was used for all other values of $[H_2O_2]$ for a given mutant.

RESULTS

Design and Characterization of A147M and A147Y. Molecular modeling based on the crystal structure of CCP [Goodin & McRee, 1993; cf. Finzel et al. (1984)] suggests that replacement of Ala-147 with a larger amino acid should partially block solvent access to the heme. Ala-147 lies at the beginning of an irregular turn between a segment of extended chain and the start of helix E (residues 150−158) on the surface of the enzyme. The peptide backbone atoms of the extended chain (residues 144−148) form part of the lip of the channel, which extends from the surface of the enzyme to the distal heme face and provides access for H_2O_2 to coordinate the iron during the activation of the enzyme. However, the existence of this channel also allows solvent access to the heme edge at the 8-methyl and δ-meso positions. Interactions between these heme positions and small molecule substrate analogs have been proposed for horseradish peroxidase (Ortiz de Montellano, 1992), manganese peroxidase (Harris et al., 1991), and CCP (Ortiz de Montellano, 1992). Pea cytosolic ascorbate peroxidase also contains Ala at the analogous position, although the fungal and plant peroxidases contain Pro (Welinder, 1992). Pro-

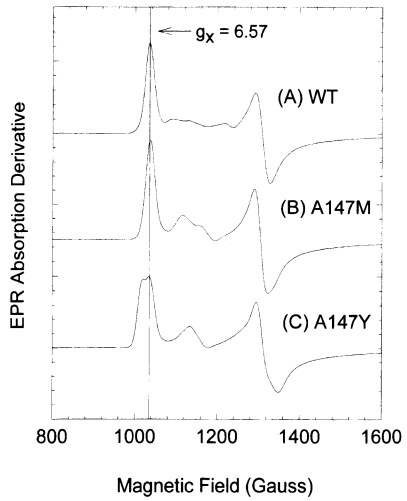

FIGURE 1: Ferric EPR spectra of CCP(MKT) (A), A147M (B), and A147Y (C). Spectra were collected in 3-mm OD quartz EPR tubes containing approximately 450 μM CCP in 100 mM potassium phosphate buffer, pH 6.0, and 50% glycerol at 7 K, 9.52-GHz microwave frequency, 20-mW microwave power, and 4.63-G modulation amplitude at 100 kHz. The arrow indicates the position for $g_x = 6.57$.

147 in lignin peroxidase is positioned about 5.0 Å from the δ-meso carbon, making the access channel in lignin peroxidase much smaller than that in CCP (Poulos et al., 1993). Interestingly, peroxidases with Pro present at this position remain able to oxidize small molecules. The C_β carbon of Ala-147 in CCP is positioned in the neck of the cavity and oriented so that the $C_\alpha - C_\beta$ vector is directed toward the 8-methyl heme substituent. These observations suggest that a larger side chain at position 147, such as Met or Tyr, would, in the absence of a large structural rearrangement, protrude into the H_2O_2 access channel and sterically hinder access to the heme edge. Of the residues which could be modeled into this position, we chose Met and Tyr over alternative residues such as Leu or Phe, not because of better packing but because they offered the potential for serving a further interesting role. As both Met and Tyr are capable of participating in radical-based one-electron oxidation reactions (Prütz et al., 1986, 1989; Larsson & Sjöberg, 1986; Debus et al., 1988; Karthein et al., 1988; Stubbe, 1989; Babcock et al., 1992), the mutants A147M and A147Y might serve either to inhibit oxidation of small molecule substrates by steric hindrance or, alternatively, to facilitate such reactions by mediating electron transfer between donor and the heme.

The A147M and A147Y mutants of CCP were constructed using site-directed mutagenesis and verified by DNA sequencing, and the mutant proteins were expressed and purified from *E. coli* as previously described (Goodin & McRee, 1993; Fitzgerald et al., 1994). The electronic structure of the heme in these mutants is very similar to that in wild-type CCP. Both A147M and A147Y exhibited UV−vis spectra essentially identical to that of wild-type CCP with the Soret maximum at 408 nm and charge transfer bands at 508 and 644 nm, indicating that these proteins contain a high-spin ferric heme. In the presence of a glassing agent, wild-type CCP exhibits a rhombically distorted high-spin ferric EPR signal ($g_x = 6.57$, $g_y = 5.26$, $g_z = 1.97$). Low-temperature EPR spectra of the ferric A147M and A147Y proteins were very similar to that observed in wild-type CCP (Figure 1). A147M displayed a signal with $g_x = 6.55$, $g_y =$

[2] The crystallographic coordinates for the structures presented in this work are available from the Protein Data Bank, Chemistry Department, Brookhaven National Laboratory, Upton, NY 11973 (Accession Numbers 3CCX and 4CCX).

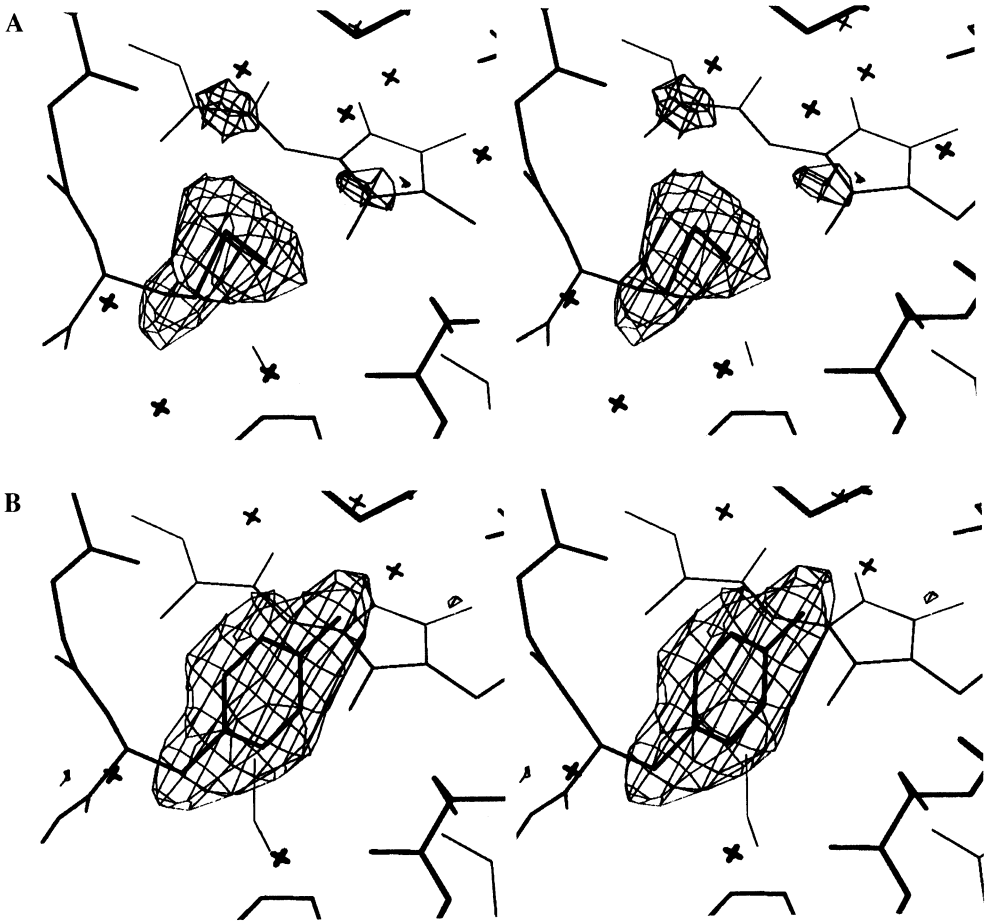

FIGURE 2: Omit maps of A147M and A147Y. Electron density contours are shown at 2σ for A147M (upper panel) and A147Y (lower panel). The residue at position 147 in each mutant structure was modeled as Gly, and $|F_o| - |F_c|$ maps were constructed after 50 cycles of positional and 15 cycles of *B*-factor refinement in X-PLOR (Brünger et al., 1987).

5.26, and $g_z = 1.97$. The spectrum for A147Y was similar, with $g_y = 5.25$ and $g_z = 1.97$, but the g_x peak was split into $g_{x1} = 6.67$ and $g_{x2} = 6.57$. This splitting suggests that the tyrosine of A147Y may slightly perturb the environment around the heme as compared to wild-type CCP.

A147M and A147Y Hinder Access to the δ-Meso Edge of the Heme. Aside from several subtle changes near the mutation site, both A147M and A147Y effectively block solvent access to the heme edge without introducing significant perturbations in the structure. Crystals of A147M and A147Y suitable for X-ray crystallographic analysis were obtained in a crystal form previously described (Wang et al., 1990; Fitzgerald et al., 1994) ($P2_12_12_1$, $a = 105.2$ Å, $b = 74.3$ Å, and $c = 45.4$ Å). X-ray crystallographic data were collected on a single crystal for each mutant. The data for A147M were integrated and scaled, resulting in a data set 80% complete to 1.9 Å resolution ($R_{sym} = 4.7$). The data for A147Y were integrated and scaled, resulting in a data set 97% complete to 2.2 Å resolution ($R_{sym} = 6.7$) (Table 1). $|F_{mutant}| - |F_{MKT}|$ difference Fourier maps constructed from the structure factors of wild-type CCP(MKT) (Goodin & McRee, 1993) indicated that structural alterations of both mutants were restricted to the region of the mutation. $|F_o| - |F_c|$ omit maps for these mutants are shown in Figure 2 in which the densities for the side chains are clearly visible. On the basis of these difference electron density maps, side chains for Met-147 and Tyr-147 were placed within the indicated electron density before several cycles of refinement/manual fitting of the side-chain dihedral angles. Refinement was further extended to the solvent model. The resulting structures for A147M and A147Y are shown in Figure 3, and Figure 4 focuses on the accessibility to the heme access channel for each structure. The side chains of both Met-

Table 1: Data Collection and Refinement Statistics[a]

	A147M	A147Y
	Data Collection	
unit cell		
a (Å)	105.2	105.2
b (Å)	74.3	74.3
c (Å)	45.4	45.4
resolution (Å)	1.9	2.2
I/σ_I (av)	16.6	10.4
I/σ_I (last shell)	1.2	1.8
no. of reflections	22774	17059
completeness (%)	80	97
R_{sym}	4.7	6.7
	Refinement	
R	0.197	0.174
resolution (Å)	5.0−1.9	5.0−2.3
no. of reflections	20182	13583
rms_{bond} (Å)	0.014	0.015
rms_{angle} (deg)	2.8	2.8
no. of waters	108	102

[a] Data were collected at 15 °C on a Siemens 4 axis area detector using Cu Kα radiation and processed as described earlier (Goodin & McRee, 1993). Each data set was collected on a single crystal, and R_{sym} represents the agreement between F_o for equivalent reflections. Values of I/σ_I (last shell) represent the average I/σ_I for the 10% of the data of highest resolution. The *R* values give the crystallographic residuals for the observed and model-derived structure factor amplitudes.

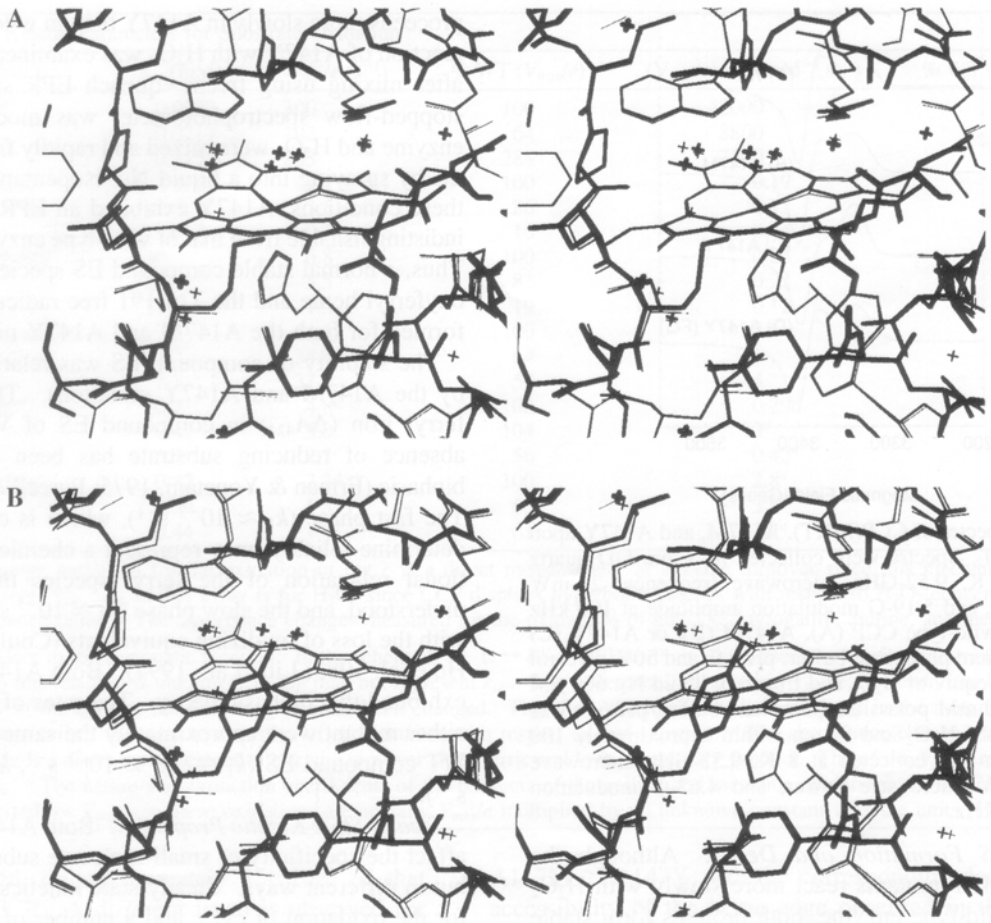

FIGURE 3: Stereoviews of the refined models for wild-type CCP, A147M, and A147Y. The upper panel compares wild-type CCP to A147M, and the lower panel compares wild-type CCP to A147Y. The wild-type CCP structure is illustrated with thin lines, and mutant structures are illustrated with thick lines.

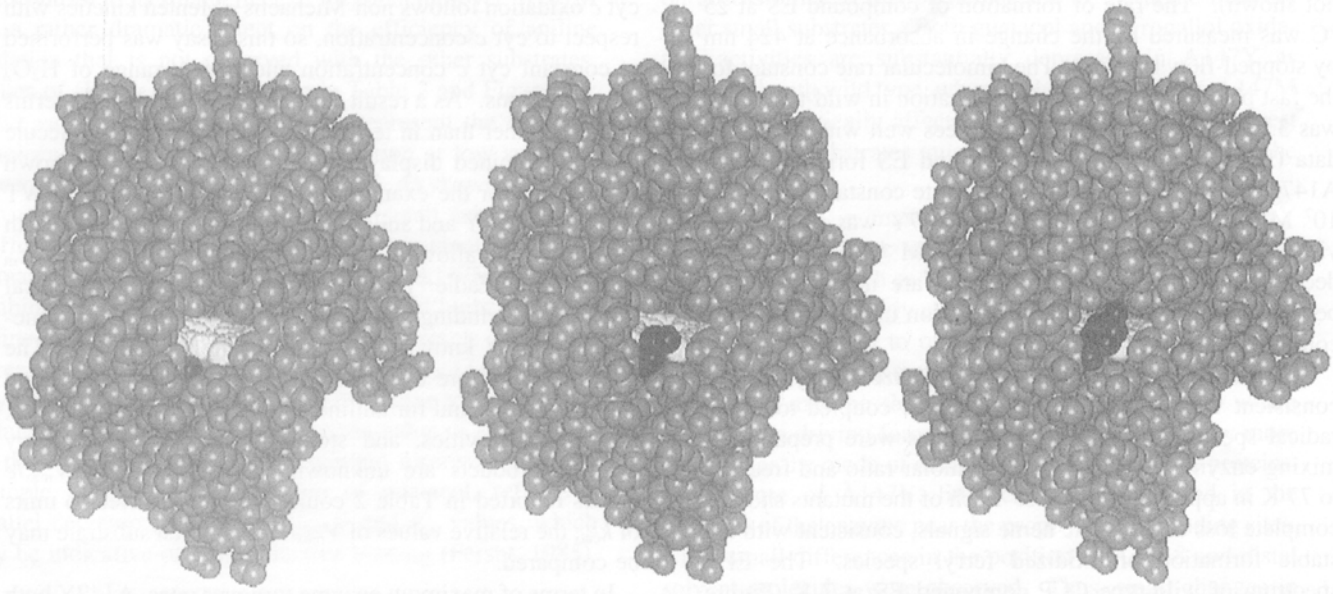

FIGURE 4: Accessibility to the heme in CCP(MKT) (left), A147M (middle), and A147Y (right). CPK models are shown without hydrogens or waters for each of the refined structures. The heme is shown in light gray, and the residue at position 147 is shown in black.

147 and Tyr-147 protrude into the heme access channel, but the channel is observed to be more effectively blocked in the A147Y mutant. Both mutants displace a water molecule which is found in the mouth of the distal cavity channel of the wild-type enzyme. In addition, several small differences exist in the distal cavity of the A147Y mutant that are not observed for A147M. A small movement of the main chain is evident from Pro-145 to Asp-148, and the side chain of Arg-48 undergoes a small shift. Possibly as a result of these changes, the solvent structure in the distal heme pocket is somewhat altered, so that two water molecules of the wild-type enzyme are replaced by a single solvent peak in A147Y. Most significantly, the water molecule closest to the heme iron, HOH-313, has moved away from the heme in A147Y. The Fe−O distance for this water increases from 2.2 Å in the wild-type enzyme to 3.3 Å in A147Y.

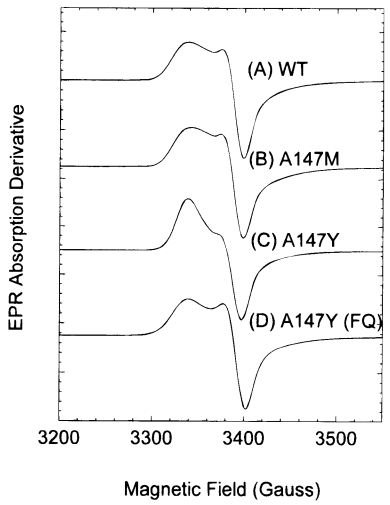

FIGURE 5: EPR spectra of CCP(MKT), A147M, and A147Y upon reaction with H_2O_2. Spectra were collected in 3-mm OD quartz EPR tubes at 7 K, 9.52-GHz microwave frequency, 20-mW microwave power, and 5.19-G modulation amplitude at 100 kHz (A–C). 450 μM wild-type CCP (A), A147M (B), or A147Y (C) in 100 mM potassium phosphate buffer, pH 6.0, and 50% glycerol was mixed with 3 equiv of H_2O_2 and frozen in liquid N_2. 600 μM A147Y (D) in 100 mM potassium phosphate buffer, pH 6.0, was mixed with 600 μM H_2O_2 and frozen within approximately 100 ms. The spectrum was collected at 8 K, 9.52-GHz microwave frequency, 20-mW microwave power, and 4.63-G modulation amplitude at 100 kHz.

Compound ES Formation and Decay. Although the A147M and A147Y mutants react more slowly with H_2O_2 than does the wild-type enzyme, both proteins form stable oxidized species. Upon addition of 1 molar equiv of H_2O_2, both mutants exhibited UV–vis spectra indistinguishable from that of compound ES of the wild-type enzyme (data not shown). The rate of formation of compound ES at 25 °C was measured by the change in absorbance at 424 nm by stopped-flow kinetics. The bimolecular rate constant for the fast phase of compound ES formation in wild-type CCP was 3.91×10^7 M^{-1} s^{-1}, which agrees well with published data (Balny et al., 1987). Compound ES formation with A147M was slightly slower, with a rate constant of 3.53×10^7 M^{-1} s^{-1}. The reaction with A147Y was slower yet, yielding a rate constant of 1.57×10^7 M^{-1} s^{-1}. These rate decreases are modest, however, and are not expected to become rate limiting for cyt *c* oxidation under steady-state conditions.

The EPR spectra for the H_2O_2-oxidized enzymes are consistent with a stable oxyferryl center coupled to a free radical species. Compound ES species were prepared by mixing enzyme and H_2O_2 in a 1:3 molar ratio and freezing to 77 K in approximately 30 s. Each of the mutants showed complete loss of the ferric heme signals, consistent with the stable formation of oxidized ferryl species. The EPR spectrum of wild-type CCP compound ES at 7 K (Figure 5A) exhibits the characteristic broad signal near $g \approx 2$ of the Trp-191 cation radical coupled to an oxyferryl heme (Sivaraja et al., 1989; Scholes et al., 1989; Houseman et al., 1993; Huyett et al., 1995). Similar signals were observed for compound ES of A147M (Figure 5B) and A147Y (Figure 5C). The small change in line shape observed for A147Y (Figure 5C) has also been observed in separate samples of wild-type CCP and was not deemed significant.

The possibility that an unstable tyrosine radical might be formed was investigated because formation of compound ES proceeds more slowly in A147Y than in wild-type CCP. The reaction of A147Y with H_2O_2 was examined at earlier times after mixing using freeze–quench EPR spectroscopy. A stopped-flow spectrophotometer was modified such that enzyme and H_2O_2 were mixed and rapidly frozen within 100 ms by spraying into a liquid N_2–isopentane slurry. Under these conditions, A147Y exhibited an EPR signal that was indistinguishable from that of wild-type enzyme (Figure 5D). Thus, a normal stable compound ES species, containing an oxyferryl heme and the Trp-191 free radical, appears to be formed for both the A147M and A147Y mutants.

The stability of compound ES was relatively unaffected by the A147M and A147Y mutations. The decay of the ferryl iron (ΔA_{424}) in compound ES of WT CCP in the absence of reducing substrate has been observed to be biphasic (Erman & Yonetani, 1975; Purcell & Erman, 1976). The fast phase ($k_1 \approx 10^{-3}$ s^{-1}), which is often difficult to determine reliably, may represent a chemical or conformational relaxation of the ferryl species that is not fully understood, and the slow phase ($k_2 \approx 10^{-5}$ s^{-1}) is associated with the loss of oxidizing equivalents (Coulson et al., 1971; Ho et al. 1983; Liu et al., 1994). Both A147M and A147Y exhibited this biphasic decay. The rates of both phases for either mutant were approximately the same as observed for WT compound ES ($k_1 = 9.8 \times 10^{-3}$ s^{-1}, $k_2 = 1.6 \times 10^{-5}$ s^{-1}).

Steady-State Kinetic Properties. Both A147M and A147Y affect the specificity of small-molecule substrate oxidation, but in different ways. Steady-state kinetics were measured for the oxidation of cyt *c* and a number of small-molecule electron donors, including aromatic phenols, amines, and a charged inorganic complex, and the kinetic parameters are presented in Table 2. As noted in Materials and Methods, cyt *c* oxidation follows non-Michaelis–Menten kinetics with respect to cyt *c* concentration, so this assay was performed at constant cyt *c* concentration and over a range of H_2O_2 concentrations. As a result, K_m values reported are in terms of H_2O_2 rather than in terms of cyt *c*. The small-molecule donors examined displayed hyperbolic kinetics, as shown in Figure 6 for the examples of guaiacol oxidation by WT CCP and A147Y and aniline oxidation by WT CCP and both mutants. This allowed the determination of V_{max}/e and K_m values from Eadie–Hofstee plots. However, for several substrates, including guaiacol, pyrogallol, aniline, and mesidine, less is known about the reaction pathways. The stoichiometries are unknown in the oxidations of guaiacol and pyrogallol, and for aniline and mesidine, the structures, molar absorptivities, and stoichiometries of the primary reaction products are unknown. Thus, while the V_{max}/e values reported in Table 2 could not be converted to units of k_{cat}, the relative values of V_{max}/e for a given substrate may be compared.

In terms of maximum enzyme turnover rates, A147Y both enhances oxidation of cyt *c* and inhibits phenolic substrate oxidation, while A147M has rather small effects for each of these substrates. As shown in Figure 7A, the maximum rate of substrate oxidation by A147Y falls into three broad groups. First, cyt *c* oxidation by this mutant is 2.9-fold higher than that observed for the WT enzyme. In the second group, oxidations of ferrocyanide and the two anilines by A147Y occur at about 50% of the maximum rate observed by WT CCP. Finally, the values of V_{max}/e for the oxidations of the two phenols, guaiacol and pyrogallol, by A147Y are

Table 2: Steady-State Kinetic Parameters for Substrate Oxidation

enzyme	substrate	K_m (mM)	V_{max}/e (s^{-1})	% WT (V_{max}/e)	$(V_{max}/e)/K_m$ (mM^{-1} s^{-1})	% WT [$(V_{max}/e)/K_m$]
wild type	cyt *c*[a]	0.0072	300	100	42000	100
A147M		0.0217	192	64	8800	21
A147Y		0.115	863	288	7500	18
wild type	guaiacol[b]	22 ± 6	4.1 ± 0.4	100	0.19	100
A147M		29 ± 5	3.5 ± 0.1	86	0.12	63
A147Y		5 ± 4	0.7 ± 0.2	16	0.14	74
wild type	pyrogallol[b]	30	6.8	100	0.23	100
A147M		25	5.5	81	0.22	96
A147Y		11	1.3	19	0.12	52
wild type	ferrocyanide[c]	7.3	54.5	100	7.5	100
A147M		3.2	34.9	64	11	147
A147Y		2.3	31.8	59	14	187
wild type	aniline[b]	16.7	4.8[d]	100	0.29[d]	100
A147M		0.42	5.0[d]	104	12[d]	4100
A147Y		6.5	2.7[d]	56	0.42[d]	145
wild type	mesidine[b]	0.82	2.3[d]	100	2.8[d]	100
A147M		0.39	1.5[d]	65	3.8[d]	136
A147Y		0.44	1.4[d]	61	3.2[d]	114

[a] The absorbance change measured for the oxidation of cyt *c* is a direct measurement of enzyme turnover since this mechanism is known. Therefore, V_{max}/e represents k_{cat}. K_m in this assay is for H_2O_2 since CCP displays hyperbolic kinetics with respect to H_2O_2 concentration but not with respect to cyt *c* concentration. [b] The absorbance changes measured for the oxidations of guaiacol, pyrogallol, aniline, and mesidine may not result from a direct product in the enzymatic reaction. In the scheme $S + E \leftrightarrow ES \xrightarrow{k_{cat}} EP \rightarrow P \xrightarrow{k_1} P^*$ we measure the formation of P*. Since the rate-determining step in this reaction is unknown, V_{max}/e may not represent k_{cat}. The differences observed in V_{max}/e, however, can be attributed to a change in the activity of the enzyme since nothing else has been changed. Therefore, the relative values of V_{max}/e in the mutants vs wild-type CCP for a given substrate reflect the relative activities of each mutant with respect to that substrate. [c] The absorbance change measured for the oxidation of ferrocyanide is a direct measurement of enzyme turnover since ferricyanide is the primary product. Therefore, V_{max}/e reported for this oxidation represents k_{cat}. [d] The nature and extinction coefficients of the products of the aniline and mesidine oxidations are uncharacterized. As a result the values reported for V_{max}/e in these oxidations are actually V_{max}/e multiplied by an unknown constant with the units mM/AU.

significantly lowered, to approximately 15−20% of that observed for WT CCP. A different trend is observed for A147M, in which aniline oxidation is slightly faster than for WT CCP (104%), while the other substrates are oxidized with maximum rates ranging from 64% to 86% of WT CCP.

In contrast to its small effect on maximal turnover, A147M has a rather dramatic effect on the efficiency of aniline oxidation that is not observed with the other substrates. Values of $(V_{max}/e)/K_m$ are shown in Table 2 and Figure 7B. These values, analogous to k_{cat}/K_m, represent the apparent bimolecular rate constant for the reaction at low substrate concentration ([S] < K_m) (Fersht, 1985). As shown in Figure 7B, values of $(V_{max}/e)/K_m$ for various small substrates are unaffected by the A147M and A147Y mutants with the dramatic exception of aniline oxidation by A147M. For this combination, $(V_{max}/e)/K_m$ is roughly 40-fold higher than for aniline oxidation by WT CCP. This is a result of a slight increase in V_{max}/e with a large decrease in K_m (Table 2) and may suggest a binding interaction of aniline to the A147M mutant. The relative constancy in the value of $(V_{max}/e)/K_m$ for the reactions with lower maximum turnover rates, for example, with A147Y oxidation of guaiacol, reflects a parallel decrease in observed V_{max}/e and K_m values, which may be indicative of nonproductive binding (Fersht, 1985).

DISCUSSION

Each of the two mutants, A147Y and A147M, have distinct effects on the specificity of substrate oxidation by the enzyme. A147Y significantly inhibits the maximal oxidation rate of both of the phenolic substrates tested, while it enhances oxidation of cyt *c*. The reduced rates observed for phenols are consistent with the proposal that these substrates are oxidized by approach to the heme edge (DePillis et al., 1991; Ortiz de Montellano, 1992). In this case, the decreasing rates observed in the order WT > A147M > A147Y with the corresponding decrease in the accessibility of the heme edge observed in the structures indicate that direct access to the heme edge is indeed a factor controlling phenol oxidation rates. The kinetic data indicate that the oxidation of phenolic substrates is more dependent on accessibility to this particular site of the heme than are other small substrates. Both guaiacol and pyrogallol oxidation activities are substantially depressed in A147Y as compared with wild type, whereas these activities in A147M are less dramatically affected. These observations suggest that phenolic substrates must approach the heme edge to be oxidized.

The increase in maximal turnover of cyt *c* by A147Y relative to wild-type enzyme was unanticipated. Other mutants of CCP, such as W51A, W51F (Goodin et al., 1991), and H175E (Choudhury et al., 1994; Smulevich et al., 1995) have been observed to oxidize cyt *c* with enhanced rates. As for these other mutations, the hyperactivity of A147Y with cyt *c* may be the result of electronic factors which enhance the driving force for electron transfer or may more subtly alter the mode of interaction between the two proteins. In the case of A147Y, little change is observed in the structure of the enzyme near the proposed cyt *c* binding sites, while small differences in the position of Arg-48 and distal solvent molecules were observed. Thus, small changes in the reactivity of the oxidized ferryl species induced by these changes cannot be excluded. It is also possible that mediated electron transfer through the tyrosine to cyt *c* is responsible, providing an alternate electron transfer pathway between the two proteins. However, no evidence for a Tyr radical was observed for A147Y by freeze−quench EPR, indicating that such a radical is either not formed or decays very rapidly.

While the A147M mutant does not have a large effect on the maximal turnover of the substrates tested, the dramatic 40-fold increase in specificity for aniline oxidation by this

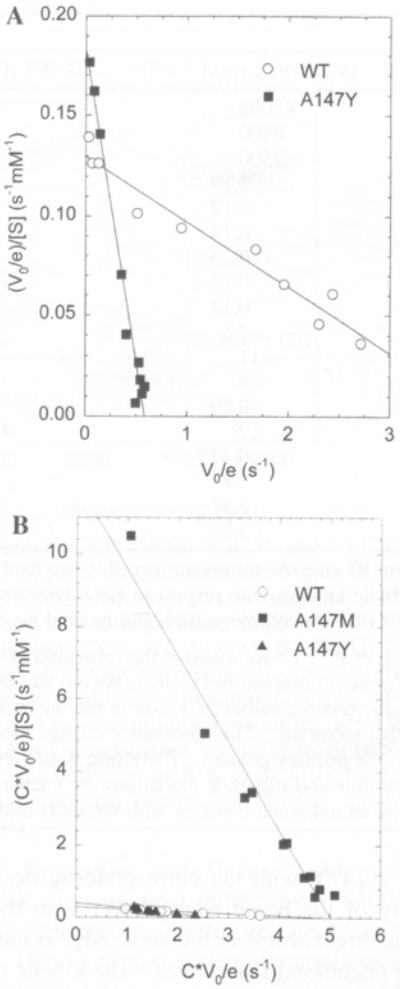

FIGURE 6: Eadie−Hofstee plots for (A) oxidation of guaiacol by wild-type CCP (○) and A147Y (■) and (B) oxidation of aniline by wild-type CCP (○),A147M (■), and A147Y (△). The lines shown are linear least-squares fits to the data. (A) 500 nM enzyme was incubated with 0.2−75 mM guaiacol and 170 μM H_2O_2 in 50 mM potassium phosphate buffer, pH 6.0. The formation of tetraguaiacol was measured at 470 nm (ϵ = 26.6 mM^{-1} cm^{-1}) (DePillis et al., 1991). (B) 1 μM enzyme was incubated with 0.1−50 mM aniline and >170 μM H_2O_2 in 100 mM potassium phosphate buffer, pH 6.0. $C*V_0/e$, where C is a constant with the units mM/AU, indicates that the values reported are proportional to V_0/e since the product of aniline oxidation is uncharacterized.

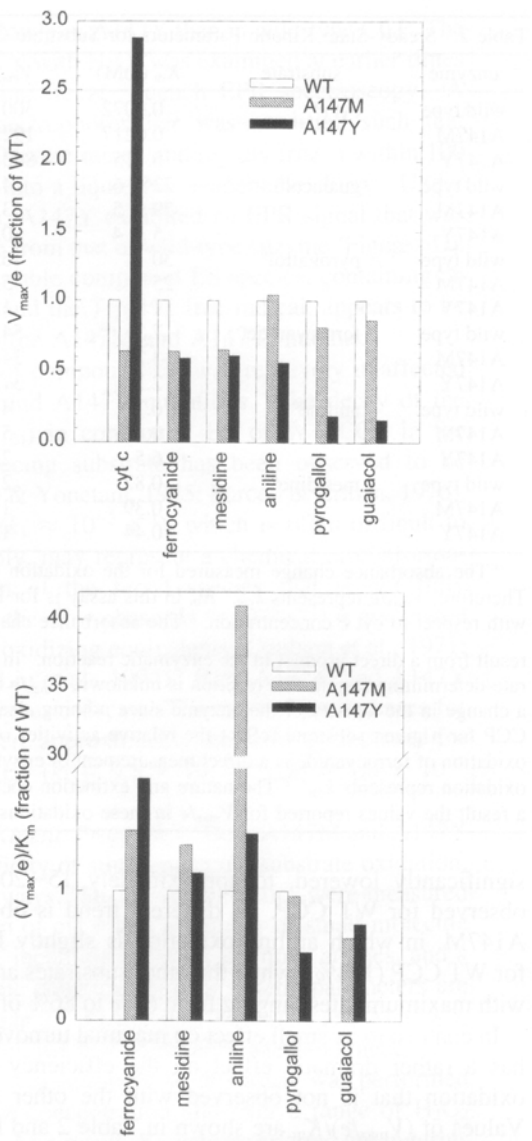

FIGURE 7: Relative CCP(MKT) (white), A147M (hatched), and A147Y (black) activities (A) and efficiencies (B) toward small molecule oxidations. Relative activities are reported as fractions of the wild-type CCP V_{max}/e for each substrate. Relative efficiencies are reported as fractions of the wild-type CCP $(V_{max}/e)/K_m$ for each substrate.

mutant suggests that a specific interaction with this substrate has been introduced. The effect on $(V_{max}/e)/K_m$ is primarily the result of a decrease in K_m. The complexity of the mechanism involving two successive reductions of compound ES prevents the direct interpretation of K_m values in terms of a specific mechanistic step. However, this parameter should be a function of each of the unimolecular events in the forward reaction pathway and thus suggests that a specific interaction between aniline and the enzyme has been introduced by the A147M mutant. A specific interaction between the methionine sulfur and the amine may stabilize binding near the heme edge for efficient electron transfer.

Ferrocyanide oxidation is not greatly affected by either of the two mutations. Both mutations decrease ferrocyanide oxidation activity to about half that of the wild-type enzyme. This observation suggests that ferrocyanide does not require unrestricted access to the heme for oxidation and may utilize a number of pathways for reduction of the oxidized enzyme.

The results of this study confirm earlier proposals (DePillis et al., 1991; Ortiz de Montellano, 1992) that manipulating the access to the δ-meso heme edge of CCP can significantly alter the specificity of substrate oxidation. Inhibition of phenol oxidation by A147Y is consistent with a steric exclusion of phenols from the heme edge. In addition, the observations of enhanced turnover of cyt c by A147Y and increased efficiency of aniline oxidation by A147M suggest that mutations at the interface between the heme edge and the protein surface may be utilized to expand the specificity of substrate oxidation.

ACKNOWLEDGMENT

The authors thank Dr. Y. Cao, Dr. R. A. Musah, and R. J. Rosenfeld for helpful discussions and critical comments.

REFERENCES

Babcock, G. T., El-Deeb, M. K., Sandusky, P. O., Whittaker, M. M., & Whittaker, J. W. (1992) *J. Am. Chem. Soc. 114*, 3727−3734.

Balny, C., Anni, H., & Yonetani, T. (1987) *FEBS Lett. 221*, 349−354.

Brünger, A. T., Kuriyan, J., & Karplus, M. (1987) *Science 235*, 458−460.
Chance, B., & Maehly, A. C. (1955) in *Methods in Enzymology* (Colowick, S. P., & Kaplan, N. O., Eds.) Vol. 2, pp 764−775, Academic Press, Inc., New York, NY.
Choudhury, K., Sundaramoorthy, M., Hickman, A., Yonetani, T., Woehl, E., Dunn, M. F., & Poulos, T. L. (1994) *J. Biol. Chem. 269*, 20239−20249.
Coulson, A. F. W., Erman, J. E., & Yonetani, T. (1971) *J. Biol. Chem. 246*, 917−924.
Debus, R. J., Barry, B. A., Babcock, G. T., & McIntosh, L. (1988) *Proc. Natl. Acad. Sci. U.S.A. 85*, 427−430.
DePillis, G. D., Sishta, B. P., Mauk, A. G., & Ortiz de Montellano, P. R. (1991) *J. Biol. Chem. 266*, 19334−19341.
Erman, J. E., & Yonetani, T. (1975) *Biochim. Biophys. Acta 393*, 350−357.
Erman, J. E., Vitello, L. B., Mauro, J. M., & Kraut, J. (1989) *Biochemistry 28*, 7992−7995.
Fersht, A. (1985) *Enzyme Structure and Mechanism*, 2nd ed., W. H. Freeman and Co., New York, NY.
Finzel, B. C., Poulos, T. L., & Kraut, J. (1984) *J. Biol. Chem. 259*, 13027−13036.
Fitzgerald, M. M., Churchill, M. J., McRee, D. E., & Goodin, D. B. (1994) *Biochemistry 33*, 3807−3818.
Fitzgerald, M. M., Trester, M. L., Jensen, G. M., McRee, D. E., & Goodin, D. B. (1995) *Protein Sci. 4*, 1844−1850.
George, P. (1952) *Nature 169*, 612−613.
George, P. (1953) *Biochem. J. 54*, 267−276.
Goodin, D. B., & McRee, D. E. (1993) *Biochemistry 32*, 3313−3324.
Goodin, D. B., Mauk, A. G., & Smith, M. (1987) *J. Biol. Chem. 262*, 7719−7724.
Goodin, D. B., Davidson, M. G., Roe, J. A., Mauk, A. G., & Smith, M. (1991) *Biochemistry 30*, 4953−4962.
Harris, R. Z., Wariishi, H., Gold, M. H., & Ortiz de Montellano, P. R. (1991) *J. Biol. Chem. 266*, 8751−8758.
Ho, P. S., Hoffman, B. M., Kang, C. H, & Margoliash, E. (1983) *J. Biol. Chem. 258*, 4356−4363.
Houseman, A. L. P., Doan, P. E., Goodin, D. B., & Hoffman, B. M. (1993) *Biochemistry 32*, 4430−4443.
Howard, A. J., Nielson, C., & Xuong, N. H. (1985) in *Methods in Enzymology* (Wyckoff, H. W., Hirs, C. H. W., & Timasheff, S. N., Eds.) Vol. 114, pp 452−472, Academic Press, Inc., Orlando, FL.
Huyett, J. E., Doan, P. E., Gurbriel, R., Houseman, A. L. P., Sivaraja, M., Goodin, D. B., & Hoffman, B. M. (1995) *J. Am. Chem. Soc. 117*, 9033−9041.
Jensen, G. M., Goodin, D. B., & Bunte, S. W. (1996) *J. Phys. Chem. 100*, 954−959.
Jordi, H. C., & Erman, J. E. (1974) *Biochemistry 13*, 3734−3741.
Kang, C. H., Ferguson-Miller, S., & Margoliash, E. (1977) *J. Biol. Chem. 252*, 919−926.
Kang, C. H., Brautigan, D. L., Osheroff, N., & Margoliash, E. (1978) *J. Biol. Chem. 253*, 6502−6510.
Kang, D. S., & Erman, J. E. (1982) *J. Biol. Chem. 257*, 12775−12779.
Karthein, R., Dietz, R., Nastainczyk, W., & Ruf, H. H. (1988) *Eur. J. Biochem. 171*, 313−320.
Kim, K. L., Kang, D. S., Vitello, L. B., & Erman, J. E. (1990) *Biochemistry 29*, 9150−9159.
Larsson, A., & Sjöberg, B.-M. (1986) *EMBO J. 5*, 2037−2040.
Liu, R.-Q., Miller, M. A., Han, G. W., Hahm, S., Geren, L., Hibdon, S., Kraut, J., Durham, B., &
Millett, F. (1994) *Biochemistry 33*, 8678−8685.
Margoliash, E., & Frohwirt, N. (1959) *Biochem. J. 71*, 570−572.
McRee, D. E. (1992) *J. Mol. Graphics 10*, 44−46.
McRee, D. E., Jensen, G. M., Fitzgerald, M. M., Siegel, H. A., & Goodin, D. B. (1994) *Proc. Natl. Acad. Sci. U.S.A. 91*, 12847−12851.
Nicola, N. A., Minasian, E., Appleby, C. A., & Leach, S. J. (1975) *Biochemistry 14*, 5141−5149.
Ortiz de Montellano, P. R. (1992) *Annu. Rev. Pharmacol. Toxicol. 32*, 89−107.
Pelletier, H., & Kraut, J. (1992) *Science 258*, 1748−1755.
Poulos, T. L., & Kraut, J. (1980) *J. Biol. Chem. 255*, 10322−10330.
Poulos, T. L., & Finzel, B. C. (1984) in *Peptide and Protein Reviews* (Hearn, M. T. W., Ed.) Vol. 4, pp. 115−171, Marcel Dekker, New York, NY.
Poulos, T. L., Edwards, S. L., Wariishi, H., & Gold, M. H. (1993) *J. Biol. Chem. 268*, 4429−4440.
Prütz, W. A., Butler, J., Land, E. J., & Swallow, A. J. (1986) *Free Radical Res. Commun. 2*, 69−75.
Prütz, W. A., Butler, J., Land, E. J., & Swallow, A. J. (1989) *Int. J. Radiat. Biol. 55*, 539−556.
Purcell, W. L., & Erman, J. E. (1976) *J. Am. Chem. Soc. 98*, 7033−7037.
Schellenberg, K. A., & Hellerman, L. (1958) *J. Biol. Chem. 231*, 547−556.
Scholes, C. P., Liu, Y., Fishel, L. A., Farnum, M. F., Mauro, J. M., & Kraut, J. (1989) *Isr. J. Chem. 29*, 85−92.
Sivaraja, M., Goodin, D. B., Smith, M., & Hoffman, B. M. (1989) *Science 245*, 738−740.
Smulevich, G., Neri, F., Willemsen, O., Choudhury, K., Marzocchi, M. P., & Poulos, T. L.
Biochemistry 34, 13485−13490.
Stemp, E. D. A., & Hoffman, B. M. (1993) *Biochemistry 32*, 10848−10865.
Stubbe, J. A. (1989) *Annu. Rev. Biochem.* 58, 257−285.
Wang, Y., & Margoliash, E. (1995) *Biochemistry 34*, 1948−1958.
Wang, J. M., Mauro, J. M., Edwards, S. L., Oatley, S. J., Fishel, L. A., Ashford, V. A., Xuong, N. H., & Kraut, J. (1990) *Biochemistry 29*, 7160−7173.
Welinder, K. G. (1992) *Curr. Opin. Struct. Biol. 2*, 388−393.
Yonetani, T. (1976) in *The Enzymes* (Boyer, P. D., Ed.) Vol. 13, pp 345−361, Academic Press, Inc., New York, NY.
Yonetani, T., & Ray, G. S. (1965) *J. Biol. Chem. 240*, 4503−4508.
Yonetani, T., Schleyer, H., & Ehrenberg, A. (1966) *J. Biol. Chem. 241*, 3240−3243.
Zhou, J. S., & Hoffman, B. M. (1994) *Science 265*, 1693−1696.
Zhou, J. S., Nocek, J. M., Devan, M. L., & Hoffman, B. M. (1995) *Science 269*, 204−207.

BI952929F